SoftwareX 12 (2020) 100593

Contents lists available at ScienceDirect

SoftwareX

journal homepage: www.elsevier.com/locate/softx

Original software publication

rheed++: A C++ framework to simulation of RHEED intensity oscillations during the growth of thin epitaxial films

Andrzej Daniluk

Institute of Computer Science, Maria Curie-Skłodowska University, ul. Akademicka 9, 20-033 Lublin, Poland

ARTICLE INFO

Article history:
Received 5 July 2020
Received in revised form 3 September 2020
Accepted 4 September 2020

Keywords:
Scientific computing
Numerical simulations
Diffuse scattering
RHEED
MBE

ABSTRACT

A time-efficient, compact and flexible computer model has been developed for calculations of RHEED intensity oscillations during the growth of thin epitaxial films. The main functionality of the model is its ability to perform dynamical calculations of amplitude of the RHEED specular beam intensity oscillations as a function of growth time using the scattering potential for heteroepitaxial structures, accounting for the possible occurrence of diffuse scattering through the layer parallel to the surface. The existence of a large number of user-definable parameters make the presented model highly versatile. To validate the model, a calculated plot of the RHEED oscillation has been compared with experimental data taken from the literature. The model does not require linking to any of the existing numerical library routines.

Code metadata

Current code version	*v1.0*
Permanent link to code/repository used of this code version	https://github.com/ElsevierSoftwareX/SOFTX_2020_278
Legal Code License	*GNU GPL 3*
Code versioning system used	*None*
Software code languages, tools, and services used	*C++11*
Compilation requirements, operating environments & dependencies	*GNU GCC, Linux, Microsoft Windows*
If available Link to developer documentation/manual	
Support email for questions	andrzej.daniluk@poczta.umcs.lublin.pl

1. Motivation and significance

The phenomenon of reflection high-energy electron diffraction (RHEED) oscillations was first observed in the early 1980s [1]. Since that time RHEED has been established as the most powerful tool for studying growth and surface analysis of thin epitaxial structures prepared by molecular beam epitaxy (MBE) in ultra-high vacuum conditions (UHV). In the RHEED experiment, monochromatic high-energy electron beam (>10 keV) is directed at a small angle (< 3^0) to the surface, where it interacts strongly with atoms near the surface. Scattered de Broglie waves interfere and create a diffraction pattern on the luminescent screen in the form of streaked spots. This is due to the fact that, for such angles, the electron beam penetrates only a few topmost monolayers and the reflected intensity is usually quite high. In such experiments, the glancing angle of the incident electron beam is usually chosen in such a way so that the specular beam intensity shows periodic oscillations as a function of growth time (intensity of the chosen spot on the RHEED pattern fluctuates in a periodic manner as a result of changes of surface coverage of the growing layers). Therefore, RHEED provides qualitative and quantitative information in situ and in real time among others about surface reconstruction, growth rate, and growth mode. Although the occurrence of the strong oscillations of RHEED intensity with the growth of thin films has become an experimentally well-established fact, the origin of the RHEED intensity oscillation is still the subject of research [2–6]. In addition, the choice of the optimal approach to performing computer simulations for electron diffraction remains an open problem. In the case of an epitaxial layer with a nearly ideal crystal lattice, intensities of electron beams reflected from the surface are calculated with the employment of the multiple scattering theory [7]. However, it should be noted that during the deposition of thin layers, the arrangement of atoms on the surface in most cases is not ideal

E-mail address: andrzej.daniluk@poczta.umcs.lublin.pl.

https://doi.org/10.1016/j.softx.2020.100593

(e.g. the occurrence of Stranski–Krastanov or Volmer–Webber growth modes), therefore the use of simplified approaches can be helpful as it reduces the time complexity of calculations.

1.1. Nucleation models

There are several types of methods that are useful in studying the nucleation process of thin epitaxial layers by MBE. If the character of the potential of interaction of atoms on the surface is known, then we can trace the evolution of the system in time, solving the deterministic equations of motion. This approach is known under the name of molecular dynamics (MD) [8]. In kinetic Monte Carlo (KMC) [9] simulations, a sequence of the atoms configuration on the surface is constructed with the employment of a pseudorandom number generator (PRNG). Both these methods take explicitly into account atomistic processes such as deposition, surface diffusion, desorption, and so on. However, they are complex calculations for which in most cases it is difficult to determine the sensitivity and uniqueness of the parameters used in comparison with the RHEED experiment. Cohen et al. [10] developed several models of epitaxy (often called the birth–death models) that are based on the temporal evolution of non-linear differential equations and study the selected parameters and properties of the growing surface. These models describe the growth process in terms of the coverage ratio $0 \Leftarrow \theta_n \Leftarrow 1$ of the n molecular layers involved in the growth process. This approach is especially interesting because it leads to both qualitative and quantitative estimates [11].

1.2. Scattering potential for heterostructures

The intensity of the beam of electrons elastically scattered by the crystal can be calculated using the one-dimensional Schrödinger equation [12]:

$$\left(\frac{d^2}{dz^2} + \frac{2m_0 E}{\hbar^2}\right)\psi(z) = \frac{2m_0}{\hbar^2} U(z)\,\psi(z) \tag{1}$$

where $\hbar$ is the reduced Planck's constant, m_0 is the electron rest mass, U(z) is the one-dimensional scattering potential of the crystal, $\psi(z)$ is the electron wave function and E is the kinetic electron energy. A one-dimensional potential U(z) is found by averaging a three-dimensional potential V(r) in planes parallel to the surface of the film. Therefore, the potential U(z) may be treated as the zeroth term of a Fourier series $\sum_G V_G(z)\exp(iG\rho)$ (where ρ is the parallel component of r, G is the reciprocal lattice vector normal to the surface) determined for the potential V(r). If we assume that the crystal is contained between two planes determined by $z=z_0$ and $z=z_n$ one can write the solution $\psi(z)$ of Eq. (1) in the following form:

$$\psi(z) = \begin{cases} e^{(i\kappa_z z)} + R_0 e^{(-i\kappa_z z)} & \text{for} \quad z > z_n \\ T_0 e^{(i\kappa_z z)} & \text{for} \quad z < z_0 \end{cases}, \tag{2}$$

and

$$\kappa_z = \frac{\sqrt{2m_0 E\left(1 + \frac{E}{2m_0c^2}\right)}}{\hbar}\sin(\vartheta), \tag{3}$$

where R_0 and T_0 are the amplitudes of the reflected and transmitted waves, respectively, κ_z is the electron wave vector (z-direction) in the vacuum, and ϑ denotes the glancing angle of the incident beam. When the form of the potential U(z) is known, one can solve Eq. (1) using the numerical algorithm that has been implemented in the *rheed++* code. In this paper we show how the dynamical approach may be applied to the creation of a practical algorithm to calculate the variation in specularly reflected beam intensity during the growth of thin epitaxial films.

RHEED specular beam intensity oscillations are calculated within the framework of the general matrix formulation detailed described in Ref. [12] under the one-beam condition. According to the one-beam condition, it is assumed that when the azimuth of the incident electron beam direction is set several degrees off from a certain crystallographic direction, fast electrons are mainly affected by the averaged potential of atomic layers parallel to the surface. The RHEED intensities are found by carrying out computations in two main stages. In the first one, the crystal slab is divided into an assembly of n monoatomic layers. Furthermore, each of these layers is divided into an assembly of i thin slices parallel to the surface assuming that each slice has a constant potential normal to the surface, and a transfer matrix is determined independently for each slice. In the second stage, having found the transfer matrices, for the top of each slice we calculate a reflectivity matrix which is determined by the relation between backward and forward traveling waves taking into account the boundary conditions for electron wave functions.

In order to theoretically elucidate the factors responsible for amplitude and RHEED oscillation changes from a growing surface the model of the one-dimensional scattering potential for heterostructures has been used [5]:

$$U(\theta, z) = \sum_i \sum_n U_n^{substrate}(\theta_n = 1, z_i) + \sum_i \sum_n \left(U_n^{layer}(\theta_n(t), z_i) + U_{add}^{layer}(\theta_n(t), z_i)\right), \tag{4}$$

where $U_n^{substrate}$ means the potential of the completely-filled substrate layers, U_n^{layer} means the potential of nth growing monolayer, U_{add}^{layer} component is responsible for diffuse scattering, $\theta_n(t)$ is the coverage of the nth surface monolayer, and z_i is the ith thin slice position along the axis perpendicular to the surface.

In order to determine the contribution of a partially full monolayer to the potential of a whole layer, the following formula is used [12]:

$$U_n^{layer}(\theta_n(t), z_i) = -\left(1 + \frac{E}{m_0c^2}\right) \times \theta_n(t) \times (1 + \alpha i) \times \frac{8\pi}{S_0} \times \sum_{k=1}^{4} \sqrt{\frac{\pi}{b_k}} a_k \times \left[\exp\left(-\frac{4\pi^2 (z_i - z_n)^2}{b_k}\right)\right], \tag{5}$$

where z_n is the nth layer position along the axis perpendicular to the surface, a_k and b_k are Doyle and Turner parameters of the analytic representation of the electron scattering factors [13], S_0 is the area of a two-dimensional unit cell parallel to the surface. The scattering potential is composed of real and imaginary parts. The real part is calculated by summing scattering contributions from individual atoms. The introduction of the imaginary part of the potential is the realization of a simplified treatment on inelastic events (core electrons, phonons and plasmons) which may happen while scattering fast electrons by the growing surface layers. It is assumed that the imaginary part of the potential is proportional to its real part and the coefficient of proportionality α is within the range $\langle 0.1; 0.2\rangle$.

The extra part of the scattering potential (4) is added to describe the random losses of electrons due to diffuse scattering by island edges [5]:

$$U_{add}^{layer}(\theta_n(t), z_i) = -\left(1 + \frac{E}{m_0c^2}\right) \times \theta_n(t) \times i\beta \times \frac{8\pi}{S_0} \times \sum_{k=1}^{4} \frac{a_k}{\sqrt{100}} \times \left[\exp\left(-\frac{4\pi^2 (z_i - z_n)^2}{100}\right)\right]. \tag{6}$$

The coefficient of proportionality β is within the range $\langle 0; 5\alpha \rangle$ and should be treated as an adjustable parameter allowing control of the magnitude of this extra potential. For $\beta = 0$ this model reduces to the proportional model of the scattering potential. For β>0 one gets an extra imaginary part of the potential. It worth noticed, that the form of potential (4) takes into account the important assumption: the diffuse scattering by island edges may seriously influence on the final shape of the oscillations. By neglecting the possibility of occurrence of diffuse scattering by island edges that being formed on the surface layer, this model reduces to the so-called proportional model of the scattering potential. A detailed discussion of the various models of the one-dimensional scattering potential along with examples of their implementation can be found in [5].

2. Software description

The open source simulation code should be easy to analyze and modify also for users for whom knowledge of high-level programming techniques is not the most important in research work. Such code should also allow considerable freedom in implementing new models. Therefore, the basic functionality of the *rheed++* is divided between two modules: *growth++* and *rheed++*. The *growth++* module can be used stand-alone and allows to carry out growth simulation for four basic models, i.e. the diffusive growth and the three variants of the distributed growth. Epitaxial growth of thin films is modeled by a set of non-linear differential equations [10,11]. The Dormand–Prince fifth-order Runge–Kutta method [14] with error estimation and adaptive stepsize control was used for solving initial value problem for non-linear differential equations [15]. The absolute and relative error tolerances and number of integration intervals are fully user-configurable.

The *growth++* reads input data from the *inputGrowthData.dat* text file where the user provides information on the parameters of the simulation of growth of thin epitaxial films. Output data are saved in the *coverage.dat* text file.

It is worth noting that in order to calculate the coverage of growing monolayers, the user can use parts of the program [11], however this requires significant code modifications.

The *rheed++* contains all the basic functions which are necessary to carry out dynamical calculations of RHEED intensity from a growing surface. The *rheed++* needs two files with input data to work properly. The first one (*inputRheedData.dat*) contains the simulation parameters of the RHHED experiment, the second one (*coverage.dat*) contains layer coverage values for the selected growth model. Output data are saved in the form of three text files. The *potential.dat* file stores values of the real part of the crystalline potential for the structures under investigation. The amplitude of the RHEED specular beam intensity oscillations is saved in the file whose name contains simulation parameters. The normalized data are saved in the file with prefix *norm-*.

3. Illustrative examples

The growth of the ultrathin metallic Ag/Si(111) layers has been the subject of extensive experimental and theoretical studies for the last decades as a model non-reactive metal–semiconductor system. Over recent years, strong efforts have been directed toward control of epitaxial growth of nanostructures and coverage-dependent structural arrangements, such as ordered noble metal overlayers on semiconductor surfaces [16–18]. The most commonly observed growth mode for non-reactive metal–semiconductor interfaces is the formation of islands with varying sizes. For Ag deposition on Si(111) at low temperature, RHEED oscillations were experimentally observed indicating a quasi-layer-by-layer growth with the islands formation [16].

The arrangements simulated in this paper refer to the fcc(111) surface. They consist of 10 geometric Si(111) layers covered with 12 Ag layers in the same configuration, as the epitaxial character of growth of the metallic layers on the silicon substrate was assumed. During the numerical calculations, it was assumed that the substrate temperature was 130 K, electron energy equals 18.8 keV, and the glancing angle of the incident electron beam equals 0.3°.

3.1. Simulation of ideal layer-by-layer growth mode

The first example demonstrates the numerical simulations of the distributed growth model that is described by the following set of coupled differential equations:

$$\frac{d\theta_n}{dt} = gR_n \left[(\theta_{n-1} - \theta_n) + \alpha_n (\theta_n - \theta_{n+1}) - \alpha_{n-1} (\theta_{n-1} - \theta_n) \right], \tag{7}$$

where the parameter α_n is defined by:

$$\alpha_n = A_n \frac{d_n(\theta_n)}{d_n(\theta_n) + d_{n+1}(\theta_{n+1})}, \tag{8}$$

and

$$d_n(\theta_n) = \theta_n (1 - \theta_n)^{1/2}. \tag{9}$$

In these equations θ_n is the coverage ratio of the layer, i.e. the ratio of the number of places occupied by atoms to the total number of lattice sites (within the range 0–1), $d_n(\theta_n)$ is the perimeter of the nth film, A_n is the phenomenological parameter that measures the net rate of transfer from one monolayer to the next, and the growth rate gR_n is $1/\tau_n$, where τ_n is the growth time of nth monolayer. This model corresponds to a growth mode in which both the number and size of the nucleation sites change during film growth.

Fig. 1(a) shows the numerical solutions of Eqs. (7)–(9) with the parameters of $gR_n = 1.0$, and $A_n = 1.0$ for all n. Fig. 1(b) presents normalized RHEED intensity oscillations dynamically calculated during the ideal layer-by-layer growth of Ag on Si(111) and corresponds to the data shown in Fig. 1(a). The changes in the oscillations of RHEED intensity show the characteristic extra maxima (often called frequency doubling) of the RHEED oscillations in the atomic layer-by-layer growth mode. This phenomenon is well-known in literature [19] and is related with interference between electron waves reflected from a top growing flat monolayer surface and from the underlying flat monolayer surface.

3.2. Simulation of quasi-layer-by-layer growth mode

The second example demonstrates the numerical calculations of the intensity of the specular electron beam during the quasi layer-by-layer growth of Ag on Si(111). Fig. 2(a) shows the numerical solutions of Eqs. (7)–(9) with the parameters of $gR_{n<=2} = 1.0$, $gR_{n>=3} = 0.8$, and $A_1 = 0.9$, $A_2 = 0.6$, $A_3 = 0.9$, $A_4 = 0.9$, $A_5 = 0.8$, $A_6 = 0.7$, $A_{n>=7} = 0.6$. Fig. 2(b) presents normalized RHEED intensity oscillations dynamically calculated during the quasi layer-by-layer growth of Ag on Si(111) corresponding to the data shown in Fig. 2(a). When Ag was grown on a clean Si(111) surface, the irregular oscillations continue up to several monolayers, and then the intensity of oscillations is damped. It means that even a slight disturbance in the arrangement of atoms at the growing surface causes a disappearance of the frequency doubling.

By analyzing the data from Fig. 2(b) and comparing them with the experimental data [16], a high level of compliance of the calculations with the experiment can be observed. It should be

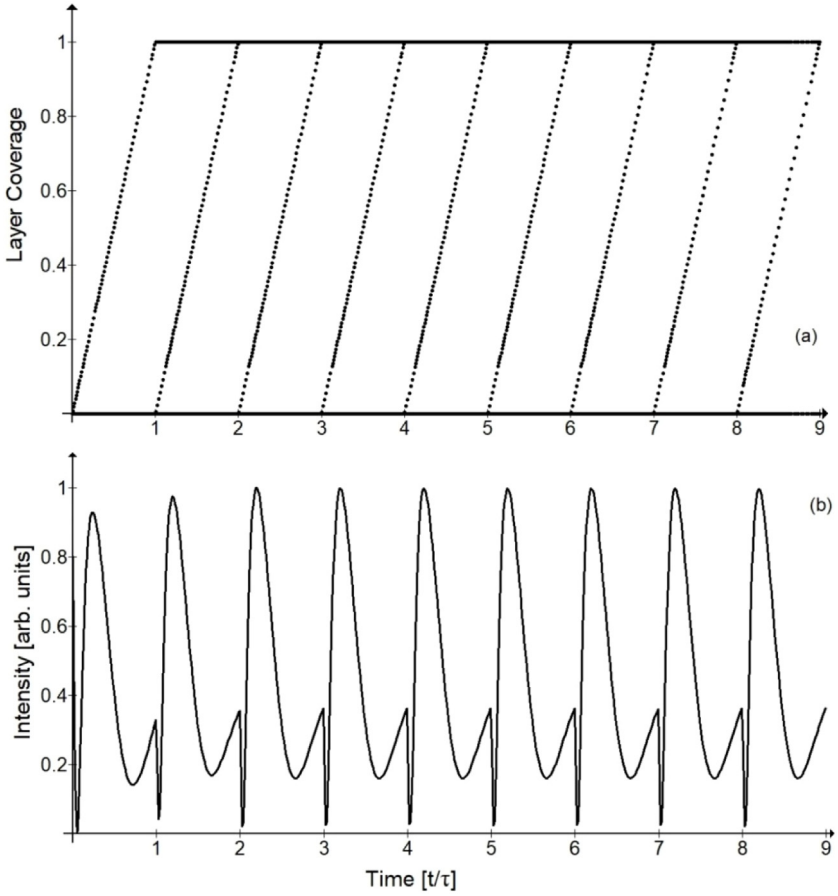

Fig. 1. (a) The surface coverage of growing layers for the atomic layer-by-layer growth mode as a function of growth time t/τ. (b) Calculated specular beam intensity oscillations corresponding to the data shown in (a). The values of the parameters $\alpha = 0.1$ and $\beta = 3\alpha$.

noted that only the unreconstructed surface of Ag is considered in this simulation, however, even for such a simplified case, the plot of the theoretical RHEED intensity oscillations reproduces the experimental results very accurately. A similar nature of changes of the RHEED intensity oscillations during the growth of Ag(111) layer on the Si(111) substrate at low temperatures and for low glancing angles of incident electron beam has been previously experimentally observed by Zhang and co-workers [20].

Fig. 3 demonstrates the dynamic change of the crystal potential [Eq. (4)] of growing layers of Ag on a clean Si(111) substrate during MBE growth, which gives rise to the reflectivity change showed in Fig. 2(b). As a result, it is considered that the RHEED oscillations are not as much due to the crystal potential shape, as due to the dynamic change of the potential depth of the growing layer.

The above examples of the practical use of the *rheed++* and *growth++* models illustrate the main computational capabilities of the presented framework. The user has the possibility to simulate the selected growth model, and then, based on the data provided by *growth++*, to simulate the changes in the intensity of the beam of electrons elastically scattered by the growing epitaxial surface layers. The possibility of numerical reproduction of the crystalline potentials of growing layers significantly facilitates the interpretation of the simulation results.

4. Impact and conclusions

Along with the development of the MBE technology, which allows the fabrication of nanostructures with a controlled composition of individual monolayers, the research attempts of many laboratories have focused on studying the dynamics of formation of both monolayers and specific heterojunction nanostructures, i.e. structures with monocrystalline interfaces formed by materials of various chemical compositions (different physicochemical properties). The fundamental scientific problem in such research is to specify both the interface type and growth mechanism for individual layers. Understanding the growth mechanisms of heteroepitaxial nanostructures is one of the main goals in solid-state physics and materials science. From a practical point of view, this knowledge is necessary to optimize the fabrication processes of optoelectronic and electronic nanodevices having specific physical properties. Nowadays, MBE laboratories (both research-oriented and commercial) are equipped with RHEED diffractometers as a standard. Therefore, researchers and technologists manufacturing heteroepitaxial nanostructures frequently use reflection high-energy electron diffraction to control the growth of samples at real time and at the atomistic level of accuracy [16,20]. This paper presents an efficient and flexible framework which facilitates the calculation of changes in the intensity of RHEED oscillations observed during the growth of thin epitaxial films. Presented models assume that in the general case one can explain qualitatively the origin of RHEED oscillations as the superposition of the following effects: (1) periodic structure of the crystal lattice with particular reference to periodic variations of the average scattering potential of the surface layer, and (2) part of the electron beam is diffuse scattering due to roughness of the surface (periodic oscillation of the size of the growing islands).

The *rheed++* is based on earlier published models used for the calculations of the RHEED rocking curves (i.e. changes in the intensity of the specular beam in the function of the glancing angle)

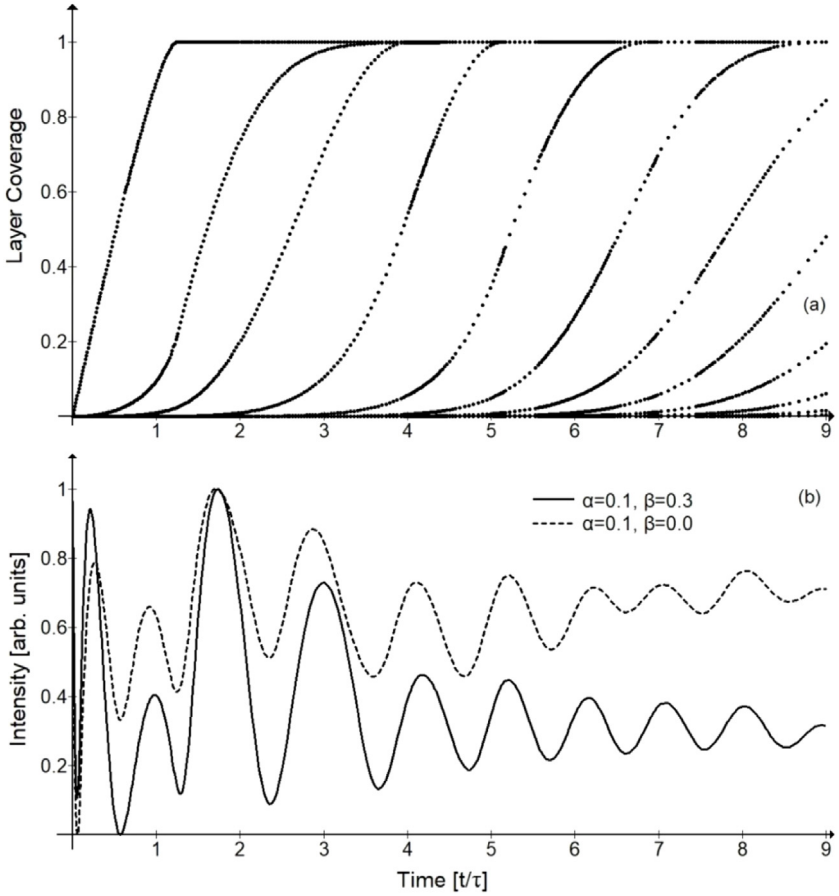

Fig. 2. (a) The surface coverage of growing layers for the quasi layer-by-layer growth mode as a function of growth time t/τ. (b) Calculated specular beam intensity oscillations corresponding to the data shown in (a). The values of the parameters α and β used in the calculations are shown in the figure.

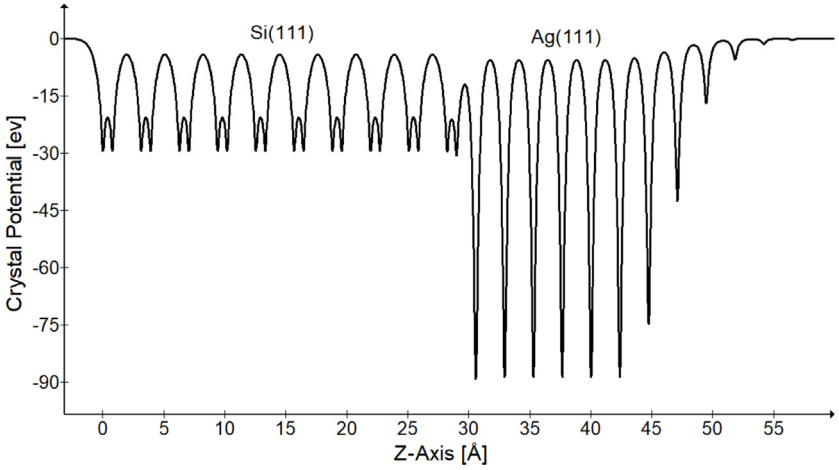

Fig. 3. The one-dimensional (real part) potential of Ag/Si(111) at 130 K for 10 bilayers thickness of Si and 12 monolayers thickness of Ag corresponds to the data shown in Fig. 2(b).

for the fixed surface [5,12]. Therefore, it can be useful as a basic framework for continued research related to solid state physics methods in the field of high-energy electron diffraction, as it can easily be modified and extended. It enables the implementation and testing of different combinations of growth models and the scattering potentials of the crystal, and can be applied to interpret experimental RHEED intensity oscillations (at least for the off-symmetry azimuths) in real time. The presented code with some modifications and properly modified input data can be applied to other crystalline structures. It should also be noted that more complex thin layer growth simulations, e.g. simulations based on KMC techniques, can be used to calculate the coverage of growing layers [21]. Linking advanced KMC techniques to the presented framework for one-beam diffraction is a very promising research perspective.

Table A.1
List of symbols used in the Eqs. (1)–(6).

Symbol	Meaning	Equivalent in the *rheed++* code
α	Coefficient of proportionality $\langle 0.1; 0.2\rangle$	alpha
β	Coefficient of proportionality $\langle 0; 5\alpha\rangle$	beta
κ_z	z-component of the electron wave vector in the vacuum	KappaZ
ϑ	Glancing angle of the incident electron beam	iAngle
E	Kinetic electron energy	E
$\hbar$	Reduced Planck's constant	hk
m_0	Rest electron mass	m0
c	Speed of light	c
t	Growth time	gt[]
$\Theta_n(t)$	Coverage of the nth monolayer	coverage[][]
$\Psi(z)$	Electron wave function	–
R_0	Amplitude of the reflected wave	R0, R0Norm[]
T_0	Amplitude of the transmitted wave	–
z_i	ith thin slice position along the axis perpendicular to the surface	Z[]
z_n	nth layer position along the axis perpendicular to the surface	Zn[]
S_0	Area of a two-dimensional unit cell parallel to the surface	S0Sub, S0Gl (Sub-substrate; Gl-growing layer)
a_k, b_k	Doyle and Turner parameters of the analytic representation of the electron scattering factors	a[], aa[], b[], bb[]
$U_n^{substrate}(1, z_i)$	Potential of the completely-filled substrate layers	Ugz[], Ug[][]
$U_n^{layer}(\Theta_n(t), z_i)$	Potential of the nth growing monolayer	Ugz[], Ug[][]
$U_{add}^{layer}(\Theta_n(t), z_i)$	Component of the potential responsible for the diffuse scattering	UgzAdd[], UgAdd[][]

Table A.2
List of symbols used in the Eqs.(7)–(9).

Symbol	Meaning	Equivalent in the *growth++* code
$\Theta_n(t)$	Coverage of the nth monolayer	theta[]
d $\Theta_n(t)$/dt	Time evolution of the coverage of the nth layer	dThetaDt[]
gR_n	Growth rate	gR[]
$d_n(\theta_n)$	Perimeter of the nth film	dnX(n, theta), where X is the symbol of the growth model
A_n	Phenomenological parameter that measures the net rate of transfer from one layer to the next	C[]

Declaration of competing interest

The authors declare that they have no known competing financial interests or personal relationships that could have appeared to influence the work reported in this paper.

Appendix

See Tables A.1 and A.2.

References

[1] Haris JJ, Joyce BA, Dobson PA. Oscillations in the surface structure of Sn-doped GaAs during growth by MBE. Surf Sci 1981;103:L90.
[2] Kawamura T, Maksym PA. RHEED Wave function and its applications. Surf Sci Rep 2009;64:122.
[3] Kawamura T, Maksym PA. Origin of RHEED intensity oscillation during homoepitaxial growth on Si(001). Surf Sci 2014;630:125.
[4] Mitura Z, Dudarev SL. Algorithms for determining the phase of RHEED oscillations. J Appl Cryst 2015;48:1927.
[5] Daniluk A. RHEED Intensities from two-dimensional heteroepitaxial nanoscale systems. Comput Phys Comm 2014;185:3001.
[6] Sun HY, Mao ZW, Zhang TW, Han L, Zhang TT, Cai XB, et al. Chemically specific termination control of oxide interfaces via layer-by-layer mean inner potential engineering. Nature Commun 2018;:9. Article (2965).
[7] Makysm PA, Beeby JL. Surf Sci, A theory of RHEED 1981;110:423.
[8] Mazzone AM. Ag deposited onto the (100) surface in silicon studied by density functional theory and classical molecular dynamics. Eur Phys J B 2003;35:517.
[9] Zhu YG, Wang TL. Kinetic Monte Carlo simulation of the initial growth of Ag thin films. Appl Surf Sci 2015;324:831.
[10] Cohen PI, Petrich GS, Pukite PR, Whaley GJ, Arrott AS. Birth-death models of epitaxy: I. Diffraction oscillations from low index surfaces. Surf Sci 1989;216:222.
[11] Daniluk A. Kinematical calculations of RHEED intensity oscillations during the growth of thin epitaxial films. Comput Phys Comm 2005;170:265.
[12] Daniluk A. Dynamical calculations for RHEED intensity oscillations. Comput Phys Comm 2005;166:123.
[13] Doyle PA, Turner PS. Relativistic Hartree–Fock X-ray and electron scattering factors. Acta Crystallogr A 1968;24:390.
[14] Dorm JR, Prince PJ. A family of embedded Runge–Kutta formulae. J Comput Appl Math 1980;6:19.
[15] Press WH, Flannery BP, Teukolsky SA, Vetterling WT. Numerical recipes the art of scientific computing. 3rd ed.. Cambridge University Press; 2007.See also, Numerical recipes in C. 2nd ed. Cambridge University Press; 1992.
[16] Zdyb R, Kopciuszyński M. Thickness-dependent spin-resolved photoemission from ultrathin Ag films on Si(111). Appl Surf Sci 2016;373:73.
[17] Bocîrnea AE, Costescu RM, Apostol NG, Teodorescu CM. Growth of Ag(111) on Si(111) with nearly flat band and abrupt interface. Appl Surf Sci 2019;473:433.
[18] Chen Y, Gramlich MW, Hayden ST, Miceli PF. Poisson-like height distribution of Ag nanoislands on Si(111)7×7. Phys Rev B 2017;95:035419.
[19] Mitura Z, Daniluk A. Studies on RHEED oscillations at low glancing angles. Surf Sci 1992;277:229.
[20] Zhang ZH, Hasegawa S, Ino S. RHEED intensity oscillation during epitaxial growth of Ag on Si(111) surfaces at low temperature. Phys Rev B 1997;55:9983.
[21] Martynec T, Klapp SHL. Modeling of nonequilibrium surface growth by a limited-mobility model with distributed diffusion length. Phys Rev E 2019;100:033307.